

Constraints on Primordial Non-Gaussianity from a Needlet Analysis of the WMAP-5 Data

Davide Pietrobon^{1,2} ^{*}, Paolo Cabella^{1,4}, Amedeo Balbi^{1,3}, Giancarlo de Gasperis¹, and Nicola Vittorio¹

¹ *Dipartimento di Fisica, Università di Roma “Tor Vergata”, via della Ricerca Scientifica 1, 00133 Roma, Italy*

² *Institute of Cosmology and Gravitation, University of Portsmouth, Mercantile House, Portsmouth PO1 2EG, United Kingdom*

³ *INFN Sezione di Roma “Tor Vergata”, via della Ricerca Scientifica 1, 00133 Roma, Italy*

⁴ *Dipartimento di Fisica, Università La Sapienza, P. le A. Moro 2, Roma, Italy*

25 October 2018

ABSTRACT

We look for a non-Gaussian signal in the WMAP 5-year temperature anisotropy maps by performing a needlet-based data analysis. We use the foreground-reduced maps obtained by the WMAP team through the optimal combination of the W, V and Q channels, and perform realistic non-Gaussian simulations in order to constrain the non-linear coupling parameter f_{NL} . We apply a third-order estimator of the needlet coefficients skewness and compute the χ^2 statistics of its distribution. We obtain $-80 < f_{\text{NL}} < 120$ at 95% confidence level, which is consistent with a Gaussian distribution and comparable to previous constraints on the non-linear coupling. We then develop an estimator of f_{NL} based on the same simulations and we find consistent constraints on primordial non-Gaussianity. We finally compute the three point correlation function in needlet space: the constraints on f_{NL} improve to $-50 < f_{\text{NL}} < 110$ at 95% confidence level.

Key words: cosmic microwave background – early universe – methods: data analysis.

1 INTRODUCTION

With the increasing amount of high-quality observations performed in the last decade (Hinshaw et al. (2008); Reichardt et al. (2008); Sievers et al. (2007); Wu et al. (2008); Pryke et al. (2008); Hinderks et al. (2008); Masi et al. (2006); Johnson et al. (2007)), statistical tests of the CMB temperature anisotropy pattern are getting more and more accurate. This has made possible to test one of the basic tenets of the standard cosmological scenario, i.e. that the primordial density perturbations follow a Gaussian distribution. This is a definite prediction of the simplest inflationary models (Guth 1981; Sato 1981; Linde 1982; Albrecht & Steinhardt 1982): the detection of primordial deviations from Gaussianity would be a smoking gun for more complicated implementations of the inflationary mechanism, such as those of multi-fields (Lyth & Wands 2002; Linde & Mukhanov 2006; Alabidi & Lyth 2006), ekpyrotic (Mizuno et al. 2008; Khoury 2002) or cyclic scenarios (Steinhardt & Turok 2002; Lehnert & Steinhardt 2008).

When dealing with the search for a non-Gaussian statistics in real data, two major issues have to be addressed. One has to do with the statistical tools used to analyse the data and detect deviations from Gaussianity: not only can these deviations be very subtle and elusive, but they could be generated by processes that are not directly related to the primordial density perturbations — such as unremoved astrophysical foregrounds (Cooray et al. 2008; Serra & Cooray 2008) or instrumental systematics. The other issue is theoretical, and relates to the way the non-Gaussianity is parameterised: while there is only one way to realize a Gaussian distribution, non-Gaussian statistics can be produced in countless ways. One then has to assume a non-Gaussian parameterisation which relates in some sensible way to an underlying early universe scenario.

The latter issue is usually addressed by introducing a parameter f_{NL} , which quantifies the amplitude of non-Gaussianity as a quadratic deviation with respect to the primordial Gaussian gravitational potential Φ_{L} , i.e.:

$$\Phi(x) = \Phi_{\text{L}}(x) + f_{\text{NL}} [\Phi_{\text{L}}^2(x) - \langle \Phi_{\text{L}}^2(x) \rangle] \quad (1)$$

The major advantage of this parameterisation is that, regardless of the specific underlying early universe model, it

^{*} E-mail: davide.pietrobon@roma2.infn.it

can represent the second-order approximation of any non linear deviation from Gaussianity. For an excellent review on this topic see Bartolo et al. (2004).

From the point of view of data analysis, a number of techniques have been proposed in the past few years to quantify the level of deviation from Gaussian statistics in the data. The most used one in harmonic space is the bispectrum (Luo 1994; Heavens 1998; Spergel & Goldberg 1999; Komatsu & Spergel 2001; Cabella et al. 2006). The bispectrum is defined as the three-point correlation function, and an estimate of f_{NL} through the bispectrum requires the sum over all the triangle configurations. Since this is extremely time-consuming, regardless whether the computation is performed in harmonic space or pixel space, Komatsu et al. (2005) have proposed a fast cubic estimator based on the Wiener filter matching, which reduces considerably the computational challenge. This estimator has been further developed by Creminelli et al. (2006) introducing a linear correction which allows the correct treatment of the anisotropic noise, and finally optimised (Yadav et al. 2007) and extended to polarisation measurements (Yadav et al. 2008). Recently, Yadav & Wandelt (2008) applied the cubic estimator to the WMAP 3-year data, finding a detection of a primordial non-Gaussian signal at more than 2.5 sigma. An indication of a primordial non-Gaussian signal has been also found by the WMAP collaboration in the analysis of the 5-year dataset, although with a lower confidence level (Komatsu et al. 2008). An interesting discussion on optimal and sub-optimal estimators can be found in Smith & Zaldarriaga (2006). See for further details Yu & Lu (2008) and Babich (2005).

Concerning the methods in pixel space, de Troia et al. (2007); Reichardt et al. (2008); Hikage et al. (2006); Curto et al. (2008, 2007) applied Minkowski functionals to several CMB datasets; Cabella et al. (2005) applied local curvature on WMAP 1-year data and Monteserín et al. (2006) developed scalar statistics using the Laplacian as a tool to test Gaussianity. Alternative indicators based on skewness and kurtosis have been proposed by Bernui & Reboucas (2008). Tests based on wavelets were applied to WMAP 1-year data (Vielva et al. 2004; Mukherjee & Wang 2004), and WMAP 5-year data by Curto et al. (2008) and McEwen et al. (2008). Wavelets have been also used in CMB studies (Martínez-González et al. 2002) to identify anomalies in WMAP data (McEwen et al. 2008; Wiaux et al. 2008; Cruz et al. 2008a, 2007; Vielva et al. 2007; Wiaux et al. 2006; Cruz et al. 2005; Vielva et al. 2004; Pietrobon et al. 2008), denoising (Sanz et al. 1999), point sources extraction (Cayón et al. 2000; González-Nuevo et al. 2006). Very recently Vielva & Sanz (2008) constrained primordial non-Gaussianity by means of N-point probability distribution functions.

In this work, we constrain the primordial non-Gaussianity by applying for the first time a novel rendition of spherical wavelets called *needlets* to the WMAP 5-year CMB data. The needlet construction is discussed by Narcowich et al. (2006); Baldi et al. (2006); Baldi et al. (2007); Marinucci et al. (2008); Geller & Marinucci (2008). Needlets have a number of interesting properties which make them a promising tool for CMB data analysis: they live on the sphere, without relying on any tangent plane approxima-

tion, are quasi-exponentially localised in pixel space and can be easily constructed from a filter function with a finite support in harmonic space. Combined with the specific shape of this function, this guarantees a tiny level of correlation among needlets, which are only marginally affected by the presence of sky cuts. An exhaustive discussion can be found in Pietrobon et al. (2006) and Marinucci et al. (2008). Recently, the needlet formalism has been extended to the polarisation field, as discussed by Geller et al. (2008). Here we try to test whether needlets can lead to interesting constraints on the non-Gaussian amplitude, when compared to previous estimates of f_{NL} .

This paper is organised as follows: in Sec. 2 we review the needlets formalism; in Sec. 3 we describe the statistical analysis of WMAP 5-year data and the constraints on f_{NL} ; we summarise our conclusions in Sec. 4.

2 NEEDLETS FORMALISM

We perform our analysis of the non-Gaussianity of WMAP 5-year data by means of needlets. So far needlets have been successfully applied to the study of the CMB in the context of the detection of the Integrated Sachs-Wolfe effect (ISW) (Pietrobon et al. 2006), the power spectrum estimation (Cruz et al. 2008b) and the study of deviations from statistical isotropy (Pietrobon et al. 2008). We refer to the work by Marinucci et al. (2008) for details on the construction of a needlet frame and a detailed analysis of its statistical properties. Here we remind that a set of needlets has one free parameter, B , which controls the width of the filter function in harmonic space. The filter function is non-vanishing only within a certain multipole range, thus allowing to keep trace of the angular information of the signal; the specific shape of the filter function also ensures a sharp localisation in pixel space. The correlation among needlets of the same set characterised by different j is much smaller than any other wavelet-like frame found in literature so far and can be easily described analytically. These features are particularly useful when looking for weak signals, like the non-Gaussianity one, which can be hidden by sky cuts and anisotropic noise.

Formally, a needlet, ψ_{jk} , is a quadratic combination of spherical harmonics which looks like

$$\psi_{jk}(\hat{\gamma}) = \sqrt{\lambda_{jk}} \sum_{\ell} b\left(\frac{\ell}{B^j}\right) \sum_{m=-\ell}^{\ell} \bar{Y}_{\ell m}(\hat{\gamma}) Y_{\ell m}(\xi_{jk}). \quad (2)$$

where $\hat{\gamma}$ is a generic direction in the sky and ξ_{jk} refers to a cubature point on the sphere for the j resolution. The function $b(\ell/B^j)$ is the filter in ℓ -space and λ_{jk} is a cubature weight number, which, following Marinucci et al. (2008), has been set for practical purpose equal to $1/N_p$, being N_p the number of pixels in the Healpix (Górski et al. 2005) scheme for the resolution chosen. We show an example of the filter function for one set among those used in the analysis in Fig. 1. In the following we use the short notation b_{ℓ} for the filter function. For a given field defined on the sphere, $T(\hat{\gamma})$,

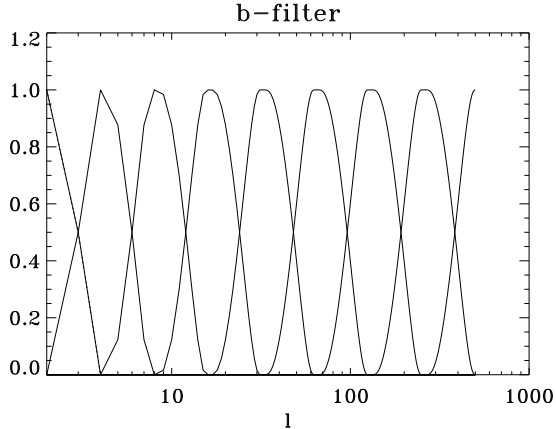


Figure 1. Filter function in ℓ -space which the needlet construction relies on. Set computed for $B = 2$.

the needlet coefficients are defined as

$$\begin{aligned} \beta_{jk} &= \int_{S^2} T(\hat{\gamma}) \psi_{jk}(\hat{\gamma}) d\Omega \\ &= \sqrt{\lambda_{jk}} \sum_{\ell} b\left(\frac{\ell}{Bj}\right) \sum_{m=-\ell}^{\ell} a_{\ell m} Y_{\ell m}(\xi_{jk}) \end{aligned} \quad (3)$$

One of the most interesting properties of β_{jk} which makes needlets particularly suitable for handling CMB data is the following relation:

$$\sum_{jk} \beta_{jk}^2 = \sum_{\ell} \frac{(2\ell+1)}{4\pi} C_{\ell} \quad (4)$$

which describes the square of needlet coefficients as an unbiased estimator of the angular power spectrum (Pietrobon et al. 2006; Marinucci et al. 2008). This means that even if we group multipoles and each needlet peaks at a certain multipole range the total power is conserved: this property is peculiar of the needlets and it is not shared by other wavelet constructions. Note that this is strictly true only if mask are not applied to the maps, while small differences are expected at low js if sky cuts are present. However when a rather broad and symmetric mask is applied, like in the case of Kq85 WMAP mask, the effect is very small.

The signature of non-Gaussianity appears into the higher moments of a distribution, which are no longer completely specified by the first moment (i.e. the mean value of the distribution) and the second moment (i.e. the standard deviation). For a Gaussian distribution, all odd moments are vanishing, while the even ones can be expressed in term of the first two only. We then look for a non-vanishing skewness of the distribution of the needlet coefficients, applying a cubic statistics.

3 WMAP-5 NEEDLET ANALYSIS

In the following we describe the statistical techniques and simulations used in order to constrain f_{NL} .

We started by producing simulations of non-Gaussian CMB maps with the WMAP-5 characteristics, for varying f_{NL} . For each channel [Q1, Q2, V1, V2, W1, W2, W3, W4], we used as input a realization of a simulated primordial

non-Gaussian map (Liguori et al. 2007); these maps were convolved with the respective beam window functions for each channel and a random noise realization was added to each map adopting the nominal sensitivities and number of hits provided by the WMAP team¹ (Hinshaw et al. 2008). From these single-channel maps we constructed an optimal map via Jarosik et al. (2007):

$$T(\gamma) = \sum_{ch} T_{ch}(\gamma) w_{ch}(\gamma) \quad (5)$$

where γ represents a direction on the sky (which, in practice, is identified with a specific pixel in the Healpix scheme (Górski et al. 2005)), and $w_{ch} = n_h(\gamma)/\sigma_{ch}^2 / \sum_{ch} w_{ch}$ where n_h is the number of observations of a given pixel and σ_{ch} the nominal sensitivity of the channel, estimated by WMAP team. We finally applied the WMAP mask Kq85 and degraded the resulting map to the resolution of $N = 256$. At the end of this procedure we were left with realistic Monte Carlo simulations of the CMB sky as seen from WMAP-5, containing different level of primordial non-Gaussianity parameterised by the value of f_{NL} .

Then, we extracted the needlet coefficients β_{jk} from the simulated maps for a given B . For each j resolution, the needlet coefficients can be visualised as a sky map, where k is the pixel number. We calculated the skewness of the reconstructed coefficients maps over the unmasked region, as:

$$S_j = \frac{1}{\tilde{N}_p} \sum_{k'} \frac{(\beta_{jk'} - \langle \beta_{jk'} \rangle)^3}{\sigma_j^3} \quad (6)$$

where \tilde{N}_p denotes the number of pixels outside the mask and σ_j is the variance of the needlet coefficients at the j resolution. This procedure allows us to build an empirical statistical distribution of the skewness as a function of f_{NL} . Finally, we calculated the skewness from the real data of the foreground-reduced WMAP 5-year Q, V and W channels data, using the same procedure applied to the simulated maps. The comparison of the real data skewness to the simulated distributions allowed us to set limits on the non-Gaussian signal in the data.

A non-vanishing skewness represents a deviation from a Gaussian distribution and could give a fundamental handle on the physics responsible for inflation and the generation of primordial fluctuations. In general we expect the needlet coefficients to pick up signal at different angular scales as a function of both j and B , making different sets sensitive to non-Gaussianity in specific ways. This could be indeed a powerful tool when looking for imprint of specific models of non-Gaussianity. This feature is enhanced by the statistics itself we consider in our analysis. Since $S \propto \beta_{jk}^3$ we have an intrinsic modulation in the power of the cube of the needlet coefficients. Figure 2 shows this effect compared to the square of the b_{ℓ} function.

For this reason it does make sense to compute the statistics defined in Eq. 6 for several sets of needlets. In particular we employed values of B from 1.8 to 4.5, choosing the step in order to span as homogeneously as possible the entire range of multipoles $\ell = 2$ to $\ell = 500$. The set of B we have considered is [1.8, 1.9, 2.0, 2.15, 2.5, 3.0, 3.5, 4.0, 4.5]. We also tried

¹ http://lambda.gsfc.nasa.gov/product/map/dr3/m_products.cfm

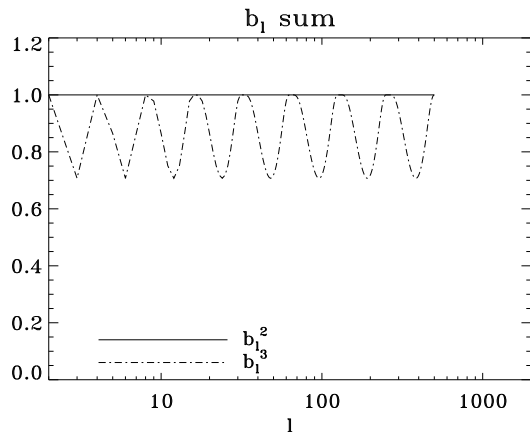


Figure 2. Solid line sum of the b_ℓ^2 ; dot-dashed line sum of the b_ℓ^3 . While the former is equal to 1 for the entire range of multipole, the latter is not.

finer samplings of B , but no additional information resulted for the sampling considered.

In Fig. 3 we report the skewness of the needlet coefficients, computed with the experimental set-up described above, for several values of B as a function of the multipole ℓ where the resolution j peaks. The curves deviating from zero corresponds to the effect due to the primordial non-Gaussianity for positive (dashed lines) and negative (dotted lines) values of f_{NL} , while the yellow and orange bands correspond to the 1σ and 2σ levels respectively. Diamonds represent the results of WMAP 5-year data.

3.1 χ^2 analysis

In order to estimate f_{NL} we minimised the quantity:

$$\chi^2(f_{\text{NL}}) = (X^d - \langle X(f_{\text{NL}}) \rangle)^T C^{-1} (X^d - \langle X(f_{\text{NL}}) \rangle). \quad (7)$$

Here X is a vector composed by the set of skewness of our set (B, j) . The averages $\langle X(f_{\text{NL}}) \rangle$ were calculated via Monte Carlo simulation over 100 primordial non-Gaussian maps. Formally, C^{-1} is dependent on f_{NL} as well but it has been shown (Spergel & Goldberg 1999; Komatsu & Spergel 2001) that for the mildly level of non-Gaussianity we expect this dependence is weak and can be estimated by Gaussian simulations. We found that calculating C^{-1} from 10000 Monte Carlo simulations gives very stable estimate.

The result is shown in Fig. 4: f_{NL} is estimated to be 20 with $-30 < f_{\text{NL}} < 70$ and $-80 < f_{\text{NL}} < 120$ at 1 and 2σ respectively. These results show no significant deviation from the Gaussian hypothesis. This is not in contrast with the values found by Yadav & Wandelt (2008), since we have performed our analysis on maps with the maximum multipole corresponding to $\ell_{\text{max}} = 500$, whereas Yadav & Wandelt (2008) clearly showed that their results crucially depend on the maximum multipole considered. The reduced χ^2 of WMAP data is 1.53 with 85 degrees of freedom.

As a further consistency check, we performed a goodness-of-fit test by calculating the quantile of the WMAP data from the non-Gaussian realizations with $f_{\text{NL}} = 20$. We found that 21% of the simulations had a larger χ^2 of the WMAP χ^2 , confirming that the specifications of our

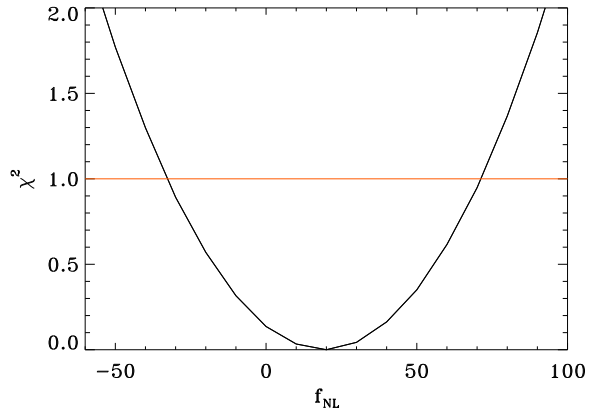


Figure 5. The $\Delta\chi^2$ of WMAP 5-year data as a function of f_{NL} . f_{NL} is estimated to be $f_{\text{NL}} = 20 \pm 50$ and $f_{\text{NL}} = 20 \pm 100$ at 1σ and 2σ level respectively.

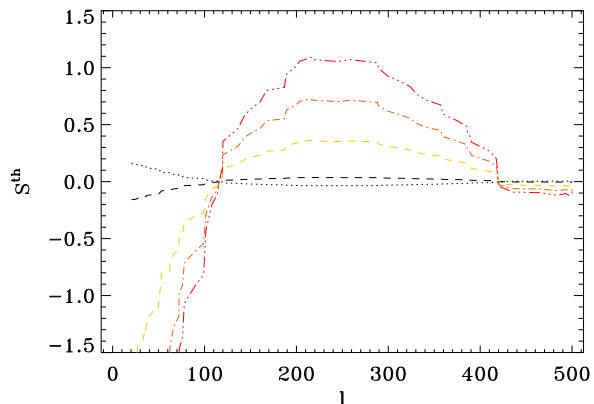


Figure 6. Skewness for $f_{\text{NL}} = \pm 1$, respectively dashed and dotted line, derived from non-Gaussian simulations. Theoretical curves for $f_{\text{NL}} = 10, 20, 30$ (from bottom to top) are shown too.

Monte Carlo simulations well describe the experimental setting of WMAP 5-year data.

3.2 A skewness based f_{NL} estimator

Since the primordial non-Gaussianity is a second order effect, it contributes linearly to the skewness through f_{NL} . This means that it is possible to compute from the non-Gaussian simulations the skewness $S(j)$ for $f_{\text{NL}} = 1$ and use it as template to build a filter-matching estimator of the non-linear coupling parameter. Assuming that $S_j^{\text{obs}} = f_{\text{NL}} S_j^{\text{th}}|_{f_{\text{NL}}=1}$, where “th” means the average over the non-Gaussian simulations, we obtain

$$f_{\text{NL}} = \frac{\sum_{jj'} S_j^{\text{obs}} \text{Cov}_{jj'}^{-1} S_{j'}^{\text{th}}}{\sum_{jj'} S_j^{\text{th}} \text{Cov}_{jj'}^{-1} S_{j'}^{\text{th}}} \quad (8)$$

where we dropped the subscript $f_{\text{NL}} = 1$. The theoretical skewness computed for $f_{\text{NL}} = 1$ is shown in Fig. 6. We checked that the pipeline applied to simulated non-Gaussian CMB maps does not affect the linear relation: in particular

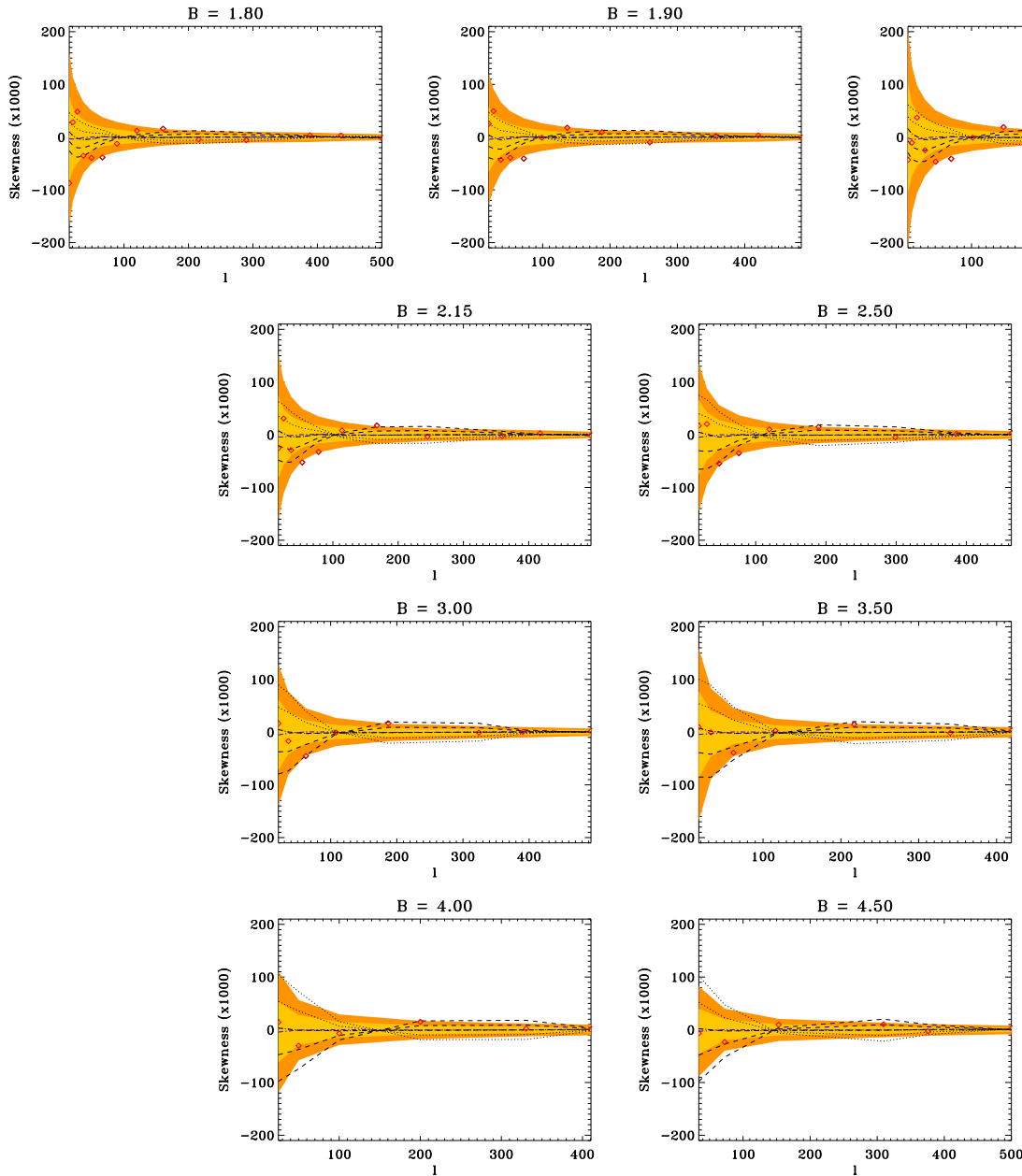


Figure 3. Skewness of needlet coefficients for different values of parameter B as a function of multipole ℓ (logarithmic function of the resolution j). Shaded areas represents 1 and 2 sigma confidence levels calculated from 10000 Gaussian Monte Carlo simulations with beam, noise level, and mask of WMAP 5-year data. Dashed (dotted) lines correspond to the averages over 100 primordial non-Gaussian maps with $f_{NL} = 200, 400$ ($-200, 400$). Diamond are the WMAP 5-year data.

we verified that the average signal we obtain for a given f_{NL} scales linearly with f_{NL} itself, meaning for example that we can mimic the signal for $f_{NL} = \pm 400$ by taking the double of that for $f_{NL} = \pm 200$.

The main contribution to the covariance matrix $\mathbf{Cov}_{jj'}$ comes from the Gaussian part of gravitational potential; this allows us to estimate the covariance from random Gaussian simulations. According to this assumption, we estimate the error bars on the primordial non-linear coupling parameter computing the standard deviation of the 10000 f_{NL} estimates resulting from a fresh set of Gaussian simulations, via Eq. 8. We find $f_{NL} = 21 \pm 54$ at 1 sigma confidence

level, which is fully consistent with what we found applying the χ^2 statistic. This corroborates the robustness of our procedure and confirms needlets as a suitable tool to study primordial non-Gaussianity.

Our limits on primordial non-Gaussianity are slightly larger than those achieved by Curto et al. (2008) being our 1σ confidence level ($-30 < f_{NL} < 70$) slightly broader than $-8 < f_{NL} < -111$ at 95% confidence level. However we were limited in our analysis to multipoles lower than $\ell_{max} = 500$, while the strongest constraints on primordial non-Gaussianity make use of higher angular scales.

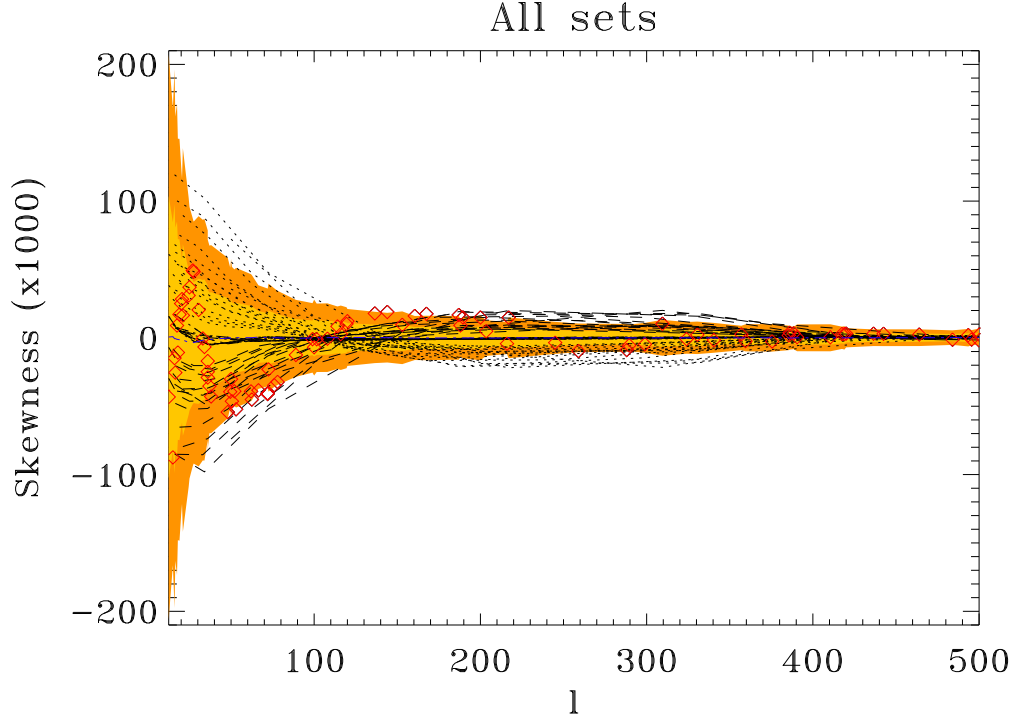


Figure 4. Skewness of needlet coefficients for the entire set of parameter B as a function of multipole ℓ . Shaded areas represents 1 and 2 σ confidence levels calculated from 10000 Gaussian Monte Carlo simulations with beam, noise level, and marks of WMAP 5-year data. Dashed (dotted) lines correspond to the averages over 100 primordial non-Gaussian maps with $f_{\text{NL}} = 200, 400$ (–200, 400). Diamond are the WMAP 5-year data.

Our limits on f_{NL} are quite promising for future experiments such as Planck², where sensitivity and angular resolution will be enormously improved.

3.3 Further analysis: binned bispectrum

The analysis we performed in the previous sections, based on the skewness of the needlets coefficients β_{jk} , is mainly sensitive to the equilateral configurations, since it is proportional to the primordial bispectrum computed for $\ell_1 \simeq \ell_2 \simeq \ell_3$ summed over all the multipoles up to $\ell_{\text{max}} = 500$. This can be easily understood by direct inspection of Eq. 6:

$$\begin{aligned}
 S_j &\simeq \frac{1}{\tilde{N}_p} \sum_k \frac{\beta_{jk}^3}{\sigma_j} \\
 &\propto \sum_{\ell_1 m_1} \sum_{\ell_2 m_2} \sum_{\ell_3 m_3} b_{\ell_1}^{(j)} b_{\ell_2}^{(j)} b_{\ell_3}^{(j)} a_{\ell_1 m_1} a_{\ell_2 m_2} a_{\ell_3 m_3} \\
 &\quad \sum_k Y_{\ell_1 m_1}(\xi_{jk}) Y_{\ell_2 m_2}(\xi_{jk}) Y_{\ell_3 m_3}(\xi_{jk}) \quad (9)
 \end{aligned}$$

The sum over pixels approximates Gaunt's integral

$$\begin{aligned}
 &\sum_k Y_{\ell_1 m_1}(\xi_{jk}) Y_{\ell_2 m_2}(\xi_{jk}) Y_{\ell_3 m_3}(\xi_{jk}) \\
 &\approx \int_S d\Omega Y_{\ell_1 m_1}(\hat{\gamma}) Y_{\ell_2 m_2}(\hat{\gamma}) Y_{\ell_3 m_3}(\hat{\gamma}) \\
 &= \sqrt{\frac{(2\ell_1 + 1)(2\ell_2 + 1)(2\ell_3 + 1)}{4\pi}} \\
 &\quad \begin{pmatrix} \ell_1 & \ell_2 & \ell_3 \\ 0 & 0 & 0 \end{pmatrix} \\
 &\quad \begin{pmatrix} \ell_1 & \ell_2 & \ell_3 \\ m_1 & m_2 & m_3 \end{pmatrix} \quad (10)
 \end{aligned}$$

and introducing the estimated bispectrum as the average over m_1, m_2 and m_3

$$\begin{aligned}
 \hat{B}_{\ell_1 \ell_2 \ell_3} &\equiv \langle a_{\ell_1 m_1} a_{\ell_2 m_2} a_{\ell_3 m_3} \rangle \\
 &= \sum_{m_1 m_2 m_3} \begin{pmatrix} \ell_1 & \ell_2 & \ell_3 \\ m_1 & m_2 & m_3 \end{pmatrix} a_{\ell_1 m_1} a_{\ell_2 m_2} a_{\ell_3 m_3}
 \end{aligned}$$

we obtain the following relation:

$$\begin{aligned}
 S_j &\propto \sum_{\ell_1 \ell_2 \ell_3} b_{\ell_1}^{(j)} b_{\ell_2}^{(j)} b_{\ell_3}^{(j)} \sqrt{\frac{(2\ell_1 + 1)(2\ell_2 + 1)(2\ell_3 + 1)}{4\pi}} \\
 &\quad \times \begin{pmatrix} \ell_1 & \ell_2 & \ell_3 \\ 0 & 0 & 0 \end{pmatrix} \hat{B}_{\ell_1 \ell_2 \ell_3} \quad (11)
 \end{aligned}$$

² [http://www.rssd.esa.int/SA/PLANCK/docs/Bluebook-ESA-SCI\(2005\)1.pdf](http://www.rssd.esa.int/SA/PLANCK/docs/Bluebook-ESA-SCI(2005)1.pdf)

Since the filter functions $b_{\ell_i}^{(j)}$ are computed for the same resolution j , the biggest contribution to the bispectrum comes

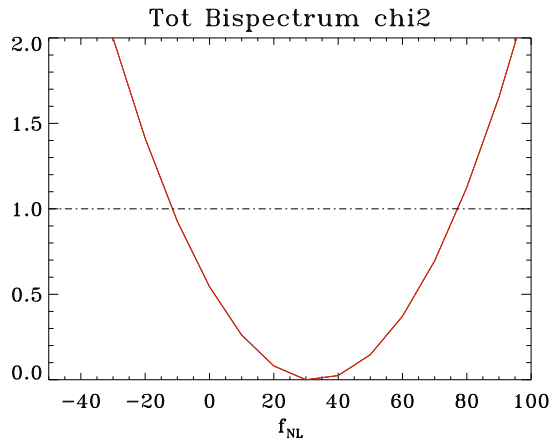


Figure 7. The $\Delta\chi^2$ of WMAP 5-year data as a function of f_{NL} computed from the binned bispectrum. B is chosen 3.50 which had the highest signal-to-noise ratio among those chosen in the previous analysis. f_{NL} is estimated to be $f_{\text{NL}} = 30 \pm 40$ and $f_{\text{NL}} = 30 \pm 80$ at 1σ and 2σ level respectively.

from the equilateral configurations, plus a smaller effect of non-equilateral triangles when, for the same j , $\ell_1 \neq \ell_2 \neq \ell_3$.

A qualitative improvement in constraining the parameter f_{NL} can be achieved by adding in the estimator the effect of the squeezed configurations, considering the product of three β_{jk} with $j_1 \neq j_2 \neq j_3$. The skewness of needlet coefficients can be generalised into

$$\begin{aligned}
 S_{j_1 j_2 j_3} &= \frac{1}{\bar{N}_p} \sum_k \frac{\beta_{j_1 k} \beta_{j_2 k} \beta_{j_3 k}}{\sigma_{j_1} \sigma_{j_2} \sigma_{j_3}} \\
 &\propto \sum_{\ell_1 \ell_2 \ell_3} b_{\ell_1}^{(j_1)} b_{\ell_2}^{(j_2)} b_{\ell_3}^{(j_3)} \sqrt{\frac{(2\ell_1 + 1)(2\ell_2 + 1)(2\ell_3 + 1)}{4\pi}} \\
 &\times \begin{pmatrix} \ell_1 & \ell_2 & \ell_3 \\ 0 & 0 & 0 \end{pmatrix} \hat{B}_{\ell_1 \ell_2 \ell_3}
 \end{aligned} \quad (12)$$

$S_{j_1 j_2 j_3}$ can be seen as a *binned bispectrum*, a smooth and combined component of the angular bispectrum.

We repeated the needlet analysis applying this new estimator to the same set of WMAP 5-year data and simulations for the choice of the needlet parameter $B = 3.5$, which has the highest signal-to-noise ratio among the set chosen in the previous analysis. The minimization of the χ^2 gives $f_{\text{NL}} = 30 \pm 40$, which is consistent with what we found applying S_j . The χ^2 for WMAP 5-year data is shown in Fig. 7

Recently an analysis based on a cubic estimator analogous to $S_{j_1 j_2 j_3}$ has been performed by Curto et al. (2008, 2009) who include the effect of squeezed configurations in the Spherical Mexican Hat Wavelet; and by Rudjord et al. (2009) using a set of needlets characterised by a different B parameter obtaining $f_{\text{NL}} = 84 \pm 40$. While the difference in the value of f_{NL} can be due to the higher number of multipoles considered in the analysis, $\ell_{\text{max}} = 1000$, and it is consistent with the result of Yadav & Wandelt (2008), it is important that the estimated error bars are fully consistent with ours.

4 CONCLUSIONS

Primordial non-Gaussianity is becoming one of the keys to understand the physics of the early Universe. Several tests have been developed and applied to WMAP data to constrain the non-linear coupling parameter f_{NL} . Recently, different methods (Yadav & Wandelt 2008; Curto et al. 2008) brought to different constraints on f_{NL} using similar datasets, WMAP 3-year and WMAP 5-year respectively. The two approaches have been shown to have the same power in constraining primordial non-Gaussianity, while they obtained different best fit values for f_{NL} . Whereas this might be due to the masks applied to the datasets, it certainly underlines the complexity and difficulty of measuring f_{NL} . The next generation of experiments will provide data with excellent angular resolution and signal-to-noise ratio which will be decisive to confirm or confute the measurements of f_{NL} of the references above. In this respect, it will be even important to constrain f_{NL} with different methods in order to get a more robust detection or to spot spurious presences of non-Gaussian signal. Moreover, integrated estimators, not based on Wiener filters, are differently sensitive to the non-linear coupling and can be useful to address exotic non-Gaussian models which predict high values of f_{NL} and whose bispectrum evaluation, for instance, may require prohibitive computational time due to the convolution in the bispectrum formula.

In this work, we constrained the primordial non-Gaussianity parameter f_{NL} by developing the needlets formalism and applying it to the WMAP 5-year CMB data. We estimated f_{NL} to be 20 with $-30 < f_{\text{NL}} < 70$ and $-80 < f_{\text{NL}} < 120$ at 1 and 2 sigma respectively, then consistent with the Gaussian hypothesis. We performed two different analyses, the χ^2 statistics and an estimator based on the skewness of the primordial non-Gaussian sky, finding an excellent agreement between the two results. Needlets have been proven to be a well understood tool for CMB data analysis, sensitive to the primordial non-Gaussianity. Since the skewness of the needlets coefficients is mainly sensitive to the equilateral triangle configurations, we improved our estimator computing the three point correlation function in needlet space which indeed recovers the signal due to squeezed triangle configurations. We obtain $f_{\text{NL}} = 30 \pm 40$ at 68% confidence level, consistent with the previous analysis. Our constraints are slightly broader than those achieved by Curto et al. (2008) and not in contrast with the values found by Yadav & Wandelt (2008) since we were limited by a smaller range of multipoles, whereas the tighter constraints on f_{NL} crucially depend on the maximum multipole considered.

Our limits on f_{NL} are quite promising for future experiments like Planck, whose sensitivity and angular resolution will be enormously improved.

ACKNOWLEDGEMENTS

We thank Frode K. Hansen, Michele Liguori and Sabino Matarrese for providing us with the primordial non-Gaussian map dataset. We are grateful to Robert Crittenden for useful discussions. We thank Domenico Marinucci for interesting discussions. D. P. thanks Asantha Cooray and the

UCI Physical Sciences Department where this work has been partially performed.

REFERENCES

- Alabidi L., Lyth D., 2006, *Journal of Cosmology and Astro-Particle Physics*, 8, 6
- Albrecht A., Steinhardt P. J., 1982, *Physical Review Letters*, 48, 1220
- Babich D., 2005, *Phys. Rev. D.*, 72, 043003
- Baldi P., Kerkyacharian G., Marinucci D., Picard D., 2006, *Annals of Statistics* in press, arXiv:math.ST/0606599
- Baldi P., Kerkyacharian G., Marinucci D., Picard D., 2007, Bernoulli in press, arXiv:0706.4169
- Bartolo N., Komatsu E., Matarrese S., Riotto A., 2004, *Phys. Rept.*, 402, 103
- Bernui A., Reboucas M. J., 2008, arXiv: 0806.3758
- Cabella P., Hansen F. K., Liguori M., Marinucci D., Matarrese S., Moscardini L., Vittorio N., 2006, *MNRAS*, 369, 819
- Cabella P., Liguori M., Hansen F. K., Marinucci D., Matarrese S., Moscardini L., Vittorio N., 2005, *MNRAS*, 358, 684
- Cayón L., Sanz J. L., Barreiro R. B., Martínez-González E., Vielva P., Toffolatti L., Silk J., Diego J. M., Argüeso F., 2000, *MNRAS*, 315, 757
- Cooray A., Sarkar D., Serra P., 2008, *Phys. Rev. D.*, 77, 123006
- Creminelli P., Nicolis A., Senatore L., Tegmark M., Zaldarriaga M., 2006, *Journal of Cosmology and Astro-Particle Physics*, 5, 4
- Cruz M., Cayón L., Martínez-González E., Vielva P., Jin J., 2007, *ApJ*, 655, 11
- Cruz M., Martínez-González E., Vielva P., Cayón L., 2005, *MNRAS*, 356, 29
- Cruz M., Martínez-González E., Vielva P., Diego J. M., Hobson M., Turok N., 2008a, *MNRAS*, 390, 913
- Cruz M., Martínez-González E., Vielva P., Diego J. M., Hobson M., Turok N., 2008b, *MNRAS*, 390, 913
- Curto A., Aumont J., Macías-Pérez J. F., Martínez-González E., Barreiro R. B., Santos D., Désert F. X., Tristram M., 2007, *A&A*, 474, 23
- Curto A., Macías-Pérez J. F., Martínez-González E., Barreiro R. B., Santos D., Hansen F. K., Liguori M., Matarrese S., 2008, *A&A*, 486, 383
- Curto A., Martínez-González E., Barreiro R. B., 2009, arXiv: 0902.1523
- Curto A., Martínez-González E., Mukherjee P., Barreiro R. B., Hansen F. K., Liguori M., Matarrese S., 2008, arXiv: 0807.0231
- de Troia G., et al. 2007, *New Astronomy Review*, 51, 250
- Geller D., Hansen F. K., Marinucci D., Kerkyacharian G., Picard D., 2008, *Phys. Rev. D.*, 78, 3533
- Geller D., Marinucci D., 2008, arXiv: 0811.2935
- González-Nuevo J., Argüeso F., López-Caniego M., Toffolatti L., Sanz J. L., Vielva P., Herranz D., 2006, *MNRAS*, 369, 1603
- Górski K. M., Hivon E., Banday A. J., Wandelt B. D., Hansen F. K., Reinecke M., Bartelmann M., 2005, *ApJ*, 622, 759
- Guth A. H., 1981, *Phys. Rev. D.*, 23, 347
- Heavens A. F., 1998, *MNRAS*, 299, 805
- Hikage C., Komatsu E., Matsubara T., 2006, *ApJ*, 653, 11
- Hinderks J., et al. 2008, arXiv: 0805.1990
- Hinshaw G., et al. 2008, arXiv :0803.0732
- Jarosik N., et al. 2007, *ApJ*, 170, 263
- Johnson B. R., et al. 2007, *ApJ*, 665, 42
- Khoury J., 2002, PhD thesis, AA(PRINCETON UNIVERSITY)
- Komatsu E., Dunkley J., Nolte M. R., Bennett C. L., Gold B., Hinshaw G., Jarosik N., Larson D., Limon M., Page L., Spergel D. N., Halpern M., Hill R. S., Kogut A., Meyer S. S., Tucker G. S., Weiland J. L., Wollack E., Wright E. L., 2008, arXiv: 0803.0547, 803
- Komatsu E., Spergel D. N., 2001, *Phys. Rev. D.*, 63, 063002
- Komatsu E., Spergel D. N., Wandelt B. D., 2005, *ApJ*, 634, 14
- Lehners J.-L., Steinhardt P. J., 2008, *Phys. Rev. D.*, 77, 063533
- Liguori M., Yadav A., Hansen F. K., Komatsu E., Matarrese S., Wandelt B., 2007, *Phys. Rev. D.*, 76, 105016
- Linde A., Mukhanov V., 2006, *Journal of Cosmology and Astro-Particle Physics*, 4, 9
- Linde A. D., 1982, *Physics Letters B*, 108, 389
- Luo X., 1994, *ApJ*, 427, L71
- Lyth D. H., Wands D., 2002, *Physics Letters B*, 524, 5
- Marinucci D., Pietrobon D., Balbi A., Baldi P., Cabella P., Kerkyacharian G., Natoli P., Picard D., Vittorio N., 2008, *MNRAS*, 383, 539
- Martínez-González E., Gallegos J. E., Argüeso F., Cayón L., Sanz J. L., 2002, *MNRAS*, 336, 22
- Masi S., et al. 2006, *A&A*, 458, 687
- McEwen J. D., Hobson M. P., Lasenby A. N., Mortlock D. J., 2008, *MNRAS*, 388, 659
- Mizuno S., Koyama K., Vernizzi F., Wands D., 2008, in *American Institute of Physics Conference Series Vol. 1040 of American Institute of Physics Conference Series, Primordial non-Gaussianities in new ekpyrotic cosmology*. pp 121–125
- Monteserín C., Barreiro R. B., Martínez-González E., Sanz J. L., 2006, *MNRAS*, 371, 312
- Mukherjee P., Wang Y., 2004, *ApJ*, 613, 51
- Narcowich F. J., Petrushev P., Ward J. D., 2006, *SIAM J. Math. Anal.*, 38, 574
- Pietrobon D., Amblard A., Balbi A., Cabella P., Cooray A., Marinucci D., 2008, arXiv: 0809.0010
- Pietrobon D., Balbi A., Marinucci D., 2006, *Phys. Rev. D*, 74, 043524
- Pryke C., et al. 2008, arXiv: 0805.1944
- Reichardt C. L., et al. 2008, arXiv: 0801.1491
- Rudjord O., Hansen F. K., Lan X., Liguori M., Marinucci D., Matarrese S., 2009, arXiv: 0901.3154
- Sanz J. L., Argüeso F., Cayón L., Martínez-González E., Barreiro R. B., Toffolatti L., 1999, *MNRAS*, 309, 672
- Sato K., 1981, *MNRAS*, 195, 467
- Serra P., Cooray A., 2008, *Phys. Rev. D.*, 77, 107305
- Sievers J. L., et al. 2007, *ApJ*, 660, 976
- Smith K. M., Zaldarriaga M., 2006, arXiv:astro-ph/0612571
- Spergel D. N., Goldberg D. M., 1999, *Phys. Rev. D.*, 59, 103001
- Steinhardt P. J., Turok N., 2002, *Science*, 296, 1436
- Vielva P., Martínez-González E., Barreiro R. B., Sanz J. L.,

- Cayón L., 2004, ApJ, 609, 22
Vielva P., Sanz J. L., 2008, arXiv: 0812.1756
Vielva P., Wiaux Y., Martínez-González E., Vandergheynst P., 2007, MNRAS, 381, 932
Wiaux Y., Vielva P., Barreiro R. B., Martínez-González E., Vandergheynst P., 2008, MNRAS, 385, 939
Wiaux Y., Vielva P., Martínez-González E., Vandergheynst P., 2006, Physical Review Letters, 96, 151303
Wu E. Y. S., et al. 2008, arXiv:0811.0618
Yadav A. P. S., Komatsu E., Wandelt B. D., 2007, ApJ, 664, 680
Yadav A. P. S., Komatsu E., Wandelt B. D., Liguori M., Hansen F. K., Matarrese S., 2008, ApJ, 678, 578
Yadav A. P. S., Wandelt B. D., 2008, Physical Review Letters, 100, 181301
Yu B., Lu T., 2008, Phys. Rev. D., 78, 063008